



Factors that influence surface PM_{2.5} values inferred from satellite observations: perspective gained for the US Baltimore–Washington metropolitan area during DISCOVER-AQ

S. Crumeyrolle^{1,2,3}, G. Chen², L. Ziemba², A. Beyersdorf², L. Thornhill^{2,4}, E. Winstead^{2,4}, R. H. Moore^{1,2}, M. A. Shook^{2,4}, C. Hudgins², and B. E. Anderson²

¹NASA Postdoctoral program, Oak Ridge Associated Universities, Oak Ridge, TN 37831, USA

²NASA Langley Research Center, Hampton, VA 23681, USA

³LOA, UMR8518, CNRS, Université Lille1, Villeneuve d'Ascq, France

⁴Science Systems and Applications (SSA), Hampton, VA 23666, USA

Correspondence to: S. Crumeyrolle (suzanne.crumeyrolle@gmail.com)

Received: 29 June 2013 – Published in Atmos. Chem. Phys. Discuss.: 6 September 2013

Revised: 8 January 2014 – Accepted: 24 January 2014 – Published: 26 February 2014

Abstract. During the NASA DISCOVER-AQ campaign over the US Baltimore, MD–Washington, D.C., metropolitan area in July 2011, the NASA P-3B aircraft performed extensive profiling of aerosol optical, chemical, and microphysical properties. These in situ profiles were coincident with ground-based remote sensing (AERONET) and in situ (PM_{2.5}) measurements. Here, we use this data set to study the correlation between the PM_{2.5} observations at the surface and the column integrated measurements. Aerosol optical depth (AOD_{550 nm}) calculated with the extinction (550 nm) measured during the in situ profiles was found to be strongly correlated with the volume of aerosols present in the boundary layer (BL). Despite the strong correlation, some variability remains, and we find that the presence of aerosol layers above the BL (in the buffer layer – BuL) introduces significant uncertainties in PM_{2.5} estimates based on column-integrated measurements (overestimation of PM_{2.5} by a factor of 5). This suggests that the use of active remote sensing techniques would dramatically improve air quality retrievals. Indeed, the relationship between the AOD_{550 nm} and the PM_{2.5} is strongly improved by accounting for the aerosol present in and above the BL (i.e., integrating the aerosol loading from the surface to the top of the BuL). Since more than 15 % of the AOD values observed during DISCOVER-AQ are dominated by aerosol water uptake, the $f(\text{RH})_{\text{amb}}$ (ratio of scattering coefficient at ambient relative humidity (RH) to scattering coefficient at low RH; see Sect. 3.2) is used to study the

impact of the aerosol hygroscopicity on the PM_{2.5} retrievals. The results indicate that PM_{2.5} can be predicted within a factor up to 2 even when the vertical variability of the $f(\text{RH})_{\text{amb}}$ is assumed to be negligible. Moreover, $f(\text{RH} = 80 \%)$ and RH measurements performed at the ground may be used to estimate the $f(\text{RH})_{\text{amb}}$ during dry conditions ($\text{RH}_{\text{BL}} < 55 \%$).

1 Introduction

Atmospheric aerosol particles have important influences on global climate and ecosystem processes, depending on their physical and chemical properties. Due to numerous studies highlighting negative health effects as a result of aerosol particle exposure, more efficient abatement measures have received serious consideration (Annesi-Maesano et al., 2007). Particulate matter (PM) is classified as a criteria pollutant and air quality standards have been established addressing PM_{2.5}, which represents the total mass concentration near the surface of particles with aerodynamic diameters less than 2.5 μm. The current air quality monitoring network provides relatively sparse geographic coverage (as an example, only 6 stations are monitoring the air quality in the San Joaquin Valley (CA); Sorek-Hamerv et al., 2013) and is mostly limited to urban areas where PM_{2.5} concentrations are greatest. Improving global air quality monitoring measurement

resolution to capture small-scale variability is a necessary priority of both the scientific and policy communities.

One important step toward this goal is the use of spaceborne sensors that allow near-continuous aerosol monitoring throughout the world. Yet, the complexity and resolution of aerosol satellite retrievals, as well as uncertainties associated with cloud interference, challenge these efforts. Several studies have explored the possibility of evaluating air quality from space (Hoff and Christopher, 2009 and references therein) and report comparisons between space and ground level measurements of aerosol concentrations for Europe (Chu et al., 2003; Vidot et al., 2007; Schaap et al., 2009), Canada (Van Donkelaar et al., 2006), the United States (Wang and Christopher, 2003; Engel Cox et al., 2004; Van Donkelaar et al., 2006; Gupta and Christopher, 2009a, b), and other locations around the globe (Gupta et al., 2007; Kumar et al., 2007, 2008). Overall, these studies have attempted to relate the spaceborne column measurements of aerosol optical attenuation to surface measurements of PM_{2.5}, especially in the summertime (Engel-Cox et al., 2006; Tian and Chen, 2010) and over urban areas (Liu et al., 2005; Schaap et al., 2009). The eastern United States, in comparison to the western United States, has been shown to be a good location for ascertaining PM_{2.5} information from aerosol optical depth (AOD) due to (1) more uniform vertical distribution of aerosols, (2) chemical composition that is dominated by sulfates and (3) widely distributed anthropogenic emission sources (Engel-Cox et al., 2006).

However, the uncertainty in relating a column integrated AOD to ground-level PM_{2.5} is compounded by spatial scale and timing mismatches between the measurements. Ground measurements necessitate averaging over timescales from hourly to daily, which improves the PM_{2.5}/AOD relationship (Gupta et al., 2006) but sacrifices accuracy during strong, short-lived pollution events that may be critical for air quality predictions and assessing air quality nonattainment. In addition, spaceborne AOD retrievals over bright surfaces can lead to the overestimation of the AOD (Van Donkelaar et al., 2006) and therefore an overestimate in PM_{2.5}.

Recent field work over the United States (Al-Saadi et al., 2008) and a three-year analysis in Taiwan (Tsai et al., 2011) using airborne (high-spectral resolution lidar, HSRL) and ground-based lidar measurements (Micro-Pulse Lidar Network (MPLNET) or aerosol robotic network (AERONET)) suggest vertical distributions are helpful to normalize satellite observations of column AOD and result in dramatically improved correlation with surface PM_{2.5} observations. Although incorporating the boundary layer (BL) depth improves the AOD–PM_{2.5} relationship, elevated layers can still confound results. Several studies reported the importance of an aerosol layer above the BL since elevated aerosol layers increase the AOD but are decoupled from the surface-based aerosol measurements (Engel-Cox et al., 2006; Schafer et al., 2008; He et al., 2008). For example, He et al. (2008) found that only 64 % of the monthly mean aerosol optical depth

over Hong Kong is due to aerosols within the BL. Still, while lidar measurements have shown a promising path forward, the limited spatial and temporal coverage of current measurements make assumptions necessary to extrapolate vertical distributions over regional and global scales.

A major advantage of remote sensing techniques is that they give information about particles as they occur in the atmosphere (i.e., at ambient relative humidity (RH)), while in situ aerosol measurements, including PM_{2.5}, are generally performed at drier conditions (often RH \leq 50 %, Colaud Coen et al., 2013). The amount of water absorbed by an aerosol is a function of its dry diameter and chemical composition. Water uptake changes the ambient aerosol mass (Pilinis and Seinfeld, 1989) and the aerosol optical properties (Schuster et al., 2009) and thus the AOD (Koelemeijer et al., 2006). Currently, aerosol liquid water content is not systematically measured at the ground sites of the global atmosphere watch (GAW) network nor on a global scale, so many studies either neglect the aerosol liquid water content when parameterizing the relationship between AOD and PM_{2.5} (Kaufman et al., 2002; Liu et al., 2005; Kumar et al., 2007; Schaap et al., 2009) or use a measurements-derived dependence of extinction coefficient on relative humidity ($f(\text{RH})$) and the surface ambient RH to estimate the aerosol liquid water content throughout the atmospheric column (e.g., Tsai et al., 2011; Koelemeijer et al., 2006). Gupta and Christopher (2009a) showed that the inclusion of meteorological parameters (e.g., RH, temperature, wind speed and cloud fraction) in addition to the BL height improve the estimation of ground level PM_{2.5} from column-integrated measurement by 21 %.

Given the possible benefits and current challenges of utilizing satellite-based observations to predict ground-level particulate air quality, the NASA DISCOVER-AQ (Deriving Information on Surface Conditions from Column and Vertically Resolved Observations Relevant to Air Quality) project was designed to deploy a coordinated and complex suite of ground and airborne measurements. The DISCOVER-AQ strategy is to make systematic, colocated observations of aerosol properties by in situ and remote-sensing techniques over a large diversity of source regions in the US (Baltimore–Washington, D.C., area, in summer 2011; San Joaquin Valley, CA, in winter 2013, and Houston, TX, in summer 2013) and over surface-based monitoring stations to provide continuous measurements of criteria pollutants. Here we focus on the Baltimore, MD–Washington, D.C., metropolitan area campaign and use this data set to evaluate our ability to diagnose surface PM_{2.5} conditions from simulated satellite observations with the unique benefit of a highly systematic characterization of the vertical extent of aerosols along with a dense coverage of ground measurements. The sampling location and the platforms used are described in Sect. 2, the P-3B instrumentation and the ground-based observations are described in Sect. 3, and the methodology in Sect. 4.

In Sect. 5, the AOD-PM_{2.5} relationship is quantitatively assessed by systematically showing that (i) low-altitude airborne and ground-level aerosols and trace gases measurements can be statistically compared, (ii) changes in ground-level PM_{2.5} (i.e., mass loading, effective radius, and chemical composition) directly affect observed AOD variability, and (iii) knowledge of aerosol vertical distribution and RH are essential parameters to better constrain the derived AOD/PM_{2.5} relationship.

2 Sampling location and platforms

The success of DISCOVER-AQ relies on the systematic and concurrent observation of column-integrated, surface, and vertically resolved distributions of aerosols and trace gases relevant to air quality as they evolve throughout the day. This has been accomplished with a combination of two NASA aircraft, a P-3B and UC-12, sampling in coordination with surface networks during field campaigns over regions characterized by a wide variety of aerosol sources. This analysis focuses on measurements from the P-3B, which was equipped with in situ aerosol instruments to measure microphysical, optical, and chemical properties of aerosols. The NASA P-3B aircraft performed 14 flights of nominal 8 h duration in the Baltimore–Washington metropolitan area in July 2011.

Flight paths for the P-3B varied minimally from flight to flight, with each flight normally involving 2 to 4 vertical profiles (spirals) over each ground site (Fig. 1). The large statistical data set allows unbiased analysis of day-to-day, diurnal, spatial, and vertical variability in this region. The P-3B performed a total of 247 profiles over the area's six ground sites (43 over Beltsville, 39 over Padonia, 43 over Aldino, 38 over Fairhill, 45 over Edgewood, and 39 over Essex; see Fig. 1 for locations). The range of vertical profile sampling was mostly limited by the air traffic control restrictions. As a result, the vertical profiles are typically from 0.3 to 3.2 km (pressure altitude), except Beltsville, where the top of the profile is about 1.50 km due to the presence of a flight path frequently used.

3 Instrumentation and observations

3.1 Ground sites

The ground sites were equipped with Sun photometers within the Aerosol Robotic Network (AERONET, Holben et al., 1998), providing a direct measure of AOD at seven wavelengths (approximately 0.340, 0.380, 0.440, 0.500, 0.675, 0.870, and 1.02 μm) with an estimated uncertainty of 1–2 % (Holben et al., 2001). Beltsville, Fairhill and Edgewood were also equipped with in situ aerosol and trace gas monitors that were operated within EPA's (Environmental Protection Agency) AQS (Air Quality System) network (<http://www.epa.gov/ttn/airs/airsaqs/>). Relevant to this study are the EPA's PM_{2.5} and ozone measurements. The PM_{2.5} mass

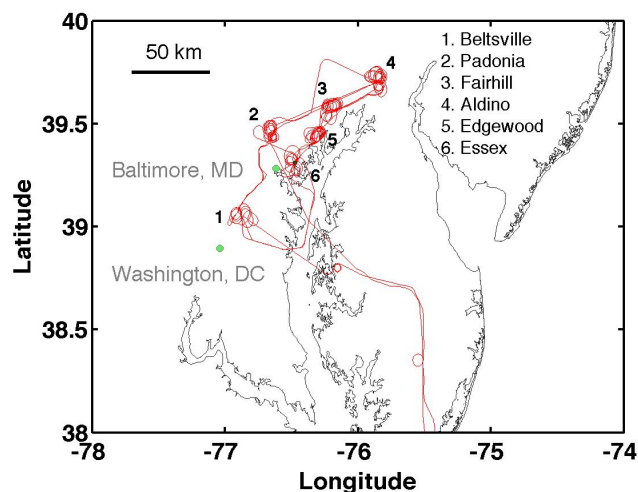


Fig. 1. Location of the DISCOVER-AQ field campaign no. 1 over Baltimore–Washington metropolitan area. The flight path followed by the P-3B is represented by the red line and the numbers correspond to the ground sites. Flight paths did not vary greatly between flights.

concentrations were measured with Met One 1020 beta attenuation monitors (BAM, Macias and Husar, 1976). The PM_{2.5} data are reported as hourly averages. The detection limit for the hourly averaged measurements is reported by the manufacturer at 4.0 μg m⁻³, and the relative uncertainty is about ± 0.1 μg m⁻³. Ozone mixing ratios were measured at each ground site by UV absorption (Gao, 2012).

3.2 Airborne (P-3B)

Aerosols were sampled through an isokinetically controlled inlet and delivered to a comprehensive suite of aerosol instruments on board the NASA P-3B aircraft. The inlet has been previously evaluated and shown to efficiently transmit particles smaller than 4 μm diameter (McNaughton et al., 2007). Simultaneous measurements of scattering (σ_{scat}) and absorption coefficients (σ_{abs}), aerosol size distribution, and aerosol chemical composition were made during DISCOVER-AQ. Dry scattering coefficient (σ_{scat}) measurements were made at 1 Hz using a three-wavelength nephelometer (TSI 3563) operating at 450, 550, and 700 nm at RH less than 40 %. The nephelometer was calibrated using filtered air and CO₂ (Anderson and Ogren, 1998) prior to, during, and after the mission. The scattering coefficient has been corrected from angular truncation errors and illumination intensity nonidealities based on Anderson and Ogren (1998). Measurements σ_{abs} were also at 1 Hz by a particle soot absorption photometer (PSAP, Radiance Research, Inc.) at 470, 532, and 660 nm wavelengths and interpolated to 550 nm using the observed Ångström exponent of absorption between 470 and 660 nm. The RH in the PSAP was not actively controlled, but filters were heated to 40 °C to reduce variability of the

measurements. PSAP data have a known scattering interference from particles deposited on the collection filter, and the measurements were post-corrected following Virkkula et al. (2010). Basic principles of filter-based measurements, like the PSAP, limit the accuracy of the observed absorption coefficient to 20 to 30 % (Ryder et al., 2013). Extinction coefficients were then calculated at dry RH (< 40 %) by summing the σ_{scat} and σ_{abs} .

Observations of particle hygroscopicity ($f(\text{RH} = 80\%)$), defined as the ratio of humidified to dry scattering coefficient, were obtained using an additional, parallel three-wavelength integrating nephelometer operating at a RH controlled at $80 \pm 4\%$. This technique is described in more detail by Ziemba et al. (2013). The sample flow routed to both nephelometers was actively dried using a nafion dryer (Perma-Pure FC-125-240-10PP), which efficiently passed accumulation mode aerosol (> 90 % transmission). Data contaminated by cloud penetrations (droplet shattering on the inlet tip) were identified visually via high particle number concentration and removed. The $f(\text{RH})_{\text{amb}}$ used to convert the measured extinction coefficient from dry ($\sigma_{\text{ext,dry}}$) to the ambient humidity conditions ($\sigma_{\text{ext,amb}}$) is defined as

$$f\text{RH}_{\text{amb}} = \frac{\sigma_{\text{ext,amb}}}{\sigma_{\text{ext,dry}}} = \left[\frac{1 - \frac{\text{RH}_{\text{amb}}}{100}}{1 - \frac{\text{RH}_{\text{dry}}}{100}} \right]^{(-\gamma)} \quad (1)$$

with

$$\gamma = \frac{\ln \left[\frac{\sigma_{\text{scat},80\%}}{\sigma_{\text{scat,dry}}} \right]}{\ln \left[\frac{100 - \text{RH}_{\text{dry}}}{100 - 80} \right]}, \quad (2)$$

where γ is an experimentally determined variable dependent on the dry and wet scattering coefficient ($\sigma_{\text{sca,dry}}$ and $\sigma_{\text{sca,wet}}$, respectively). The ambient RH measurements were performed by a hygrometer located outside the aircraft. During DISCOVER-AQ, γ varied between 0.2 and 0.7, and was inversely correlated with the organic mass fraction of the aerosol (Beyersdorf et al., 2014), consistent with the results from Quinn et al. (2005). According to the Eq. (1), the particle extinction efficiency is monotonically modified as RH increase or decrease and thus does not account for the hysteresis behavior of deliquescent aerosol particles (Fierz-Schmidhauser et al., 2010).

Recently, Ziemba et al. (2013) presented a statistical comparison of in situ extinction coefficient measurements (adjusted to 532 nm) coincident with remote-sensing observations performed by the HSRL (measured at 532 nm). It revealed good agreement (slope 1.11 and $R^2 = 0.88$) consistently over the entire ambient RH range within instrumental uncertainty. Part of this systematic difference may be due to particle losses through the inlet and the dryer (10 % losses through the dryer). This result demonstrated that (1) all the particles observed by the HSRL are within the sampling size range of the in situ measurements (i.e., particles observed

in this region are smaller than the inlet cutoff diameter of 4 μm) and (2) the parameterization (Eq. (1); Hänel (1976); Hänel (1984); Hegg et al. (1993); Tang (1996); Anderson and Ogren (1998); Carrico et al. (1998); Carrico et al. (2000); Gasso et al. (2000); Day et al. (2001)) is valid to correct observations performed at dry RH to ambient conditions.

Along with the optical measurements, dry aerosol size distributions were determined for 0.06–1.0 μm diameter particles using an ultra-high sensitivity aerosol spectrometer (UHSAS, Droplet Measurement Technologies) with a 1 Hz frequency. The UHSAS was calibrated with polystyrene latex spheres (PSL) and post-corrected with ammonium sulfate in order to provide optical particle sizing most representative of ambient aerosol. The $\sigma_{\text{scat,dry}}$ measurements were compared to modeled $\sigma_{\text{scat,dry}}$ calculated using Mie theory, the UHSAS size distribution measurements, and assuming a particle refractive index of 1.53–0.00i for ammonium sulfate (Ziemba et al., 2013). This closure exercise (slope of 0.991 ± 0.004 and r^2 of 0.98) gives confidence in both the $\sigma_{\text{scat,dry}}$ and dry size distribution measurements.

Chemical composition measurements were made with a pair of particle-into-liquid samplers (PILS). The PILS captures soluble aerosol constituents in the sampled air flow into a liquid flow of deionized water. The first PILS was coupled to a total organic carbon (TOC) analyzer (Sievers Model 800) to give the mass of the water-soluble organic carbon at a 10 s time resolution. The effluent from the second PILS was collected in 0.8 mL vials for later ion chromatographic measurement of sodium, ammonium, potassium, calcium, magnesium, chloride, nitrite, nitrate and sulfate. Sampling intervals for the inorganic analysis varied between three and five minutes.

4 Methodology

The AOD represents the integral of the ambient aerosol extinction coefficient, $\sigma_{\text{ext,amb}}$ from the surface (z_{surf}) to the top of the atmosphere (z_{TOA}):

$$\text{AOD} = \int_{z_{\text{surf}}}^{z_{\text{TOA}}} \sigma_{\text{ext,amb}}(z) dz. \quad (3)$$

Since the P-3B profile typically begins at ~ 300 m altitude, it is necessary to add the aerosol extinction between 0–300 m in order to calculate an AOD from the observed $\sigma_{\text{ext,amb}}$ (Eq. 2) for comparison with surface-base measurements. In the absence of additional aerosol sources and assuming the boundary layer is well mixed, the measurements between the aircraft and the surface should be coupled and consistent. As the P-3B measurements were performed during the summer, the BL is expected to be well mixed throughout the daytime except in the early morning before surface heating becomes a driving factor. The ozone mixing ratio is the only quasi-conserved parameter between the P-3B that is also measured

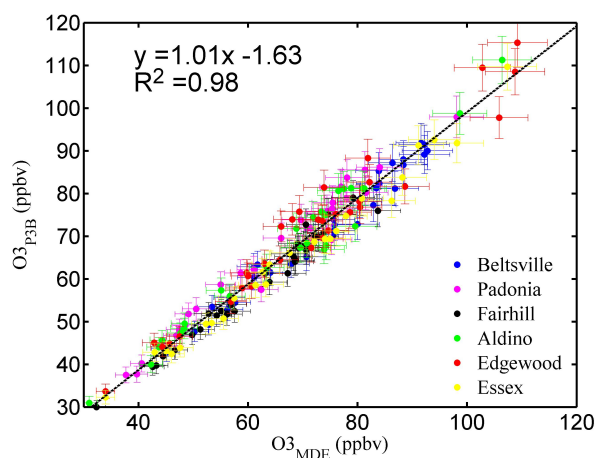


Fig. 2. Ozone measured from the EPA ground sites (at Beltsville, Padonia, Fairhill, Aldino, Edgewood and Essex) as a function of the ozone measured on-board the P-3B at the lowest level of each profile.

at each of the ground sites and is a good tracer, as it will be fairly uniform in a well-mixed boundary layer. Figure 2 shows the ozone measured at the lowest level of the P-3B profile as a function of ozone at the surface (MDE ground sites). The high correlation coefficient (0.98) and linear regression slope of 1.01 illustrate that mixing in the BL is sufficient to assume aerosol loading and properties are homogeneous from the lowest aircraft altitude to surface. Similar results were obtained for analysis of each site independently. Thus, the AOD_{P-3B} is calculated by assuming a constant $\sigma_{ext,amb}$ value between the lowest aircraft altitude to surface. The estimated portion is typically less than 16 % of the AOD_{P-3B} and any variability resulting from the assumption of constant aerosol extinction in the surface layer is likely minor.

To evaluate whether the measured AOD_{P-3B} are representative of the entire atmospheric column, values were directly compared to the AOD measured by the AERONET Sun photometers (AOD_{TOA} , see Fig. 3), which is considered as a reference for AOD measurements (Holben et al., 1998). Only profiles performed within a 1 h window of the AERONET retrievals were used in this comparison. A total of 114 profiles met these criteria. The AOD_{P-3B} was calculated using the measured scattering coefficient adjusted to 440, 500 and 675 nm using the scattering Ångström exponent and the measured absorption coefficient adjusted to the same wavelength using the absorption Ångström exponent. The comparison shows good correlation ($R^2 = 0.96$ for each wavelength), although AOD_{TOA} values are higher than the AOD_{P-3B} by nearly a factor of 1.23, based on the slope of the linear regression. Other studies have also noted that AODs calculated from in situ instrumentation and retrieved by remote sensing are well correlated, with the latter typically greater than the former (Schmid et al., 2000, 2009; Hartley et al.,

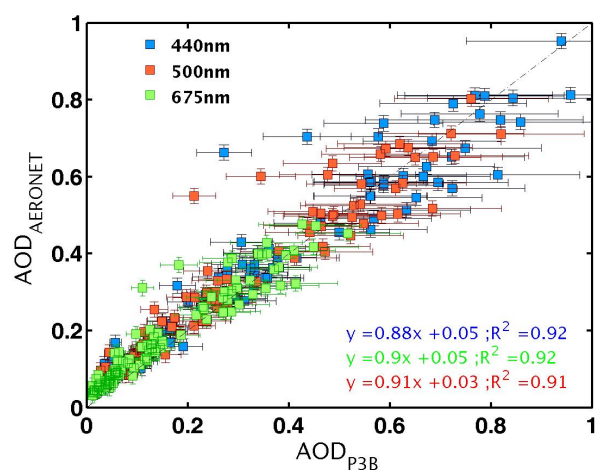


Fig. 3. AOD measured by AERONET as a function of AOD retrieved from the P-3B extinction measurements for three wavelengths (440, 500 and 675nm, respectively blue, green and red). The error bar depicts the instrumental variability for the AOD calculated from the P-3B measurements and ± 0.02 for the AOD measured by AERONET (Holben et al., 1998).

2000; Sheridan et al., 2002; Andrews et al., 2004). Esteve et al. (2012) listed the different hypotheses to explain the discrepancy between the AOD measured by AERONET and the one calculated from in situ measurements. The good agreement (discrepancy of 11 %) between the in situ and HSRL measurements allow us to estimate at 11 % the errors due to measurement adjustments (angular truncations, wavelength changes, hygroscopic growth), particle losses and underestimation of the contribution below the P-3B profile height. Thus, the larger offset (23 %) observed between the AOD from AERONET and from in situ measurements may be due to underestimation of the contribution below the P-3B profile height, the presence of an aerosol layer above the HSRL flight level (above 8.5 km), incorrect AERONET AOD cloud screening, the temporal variability of the aerosol optical properties, and a bias in the AERONET measurements.

The impact of atmospheric structure on measured AODs was examined using the temperature, relative humidity, and wind data recorded during the P-3B profiles. At least three dynamical layers are evident: the boundary layer (BL), the buffer layer (BuL) and the Free Troposphere (FT). The well-mixed, boundary layer is determined as Lenschow et al. (1999), while the BuL is the transition layer between the BL and the FT with a pronounced gradient of aerosol concentrations from the typically higher concentration observed in the BL and typically cleaner conditions observed in the FT. The use of the BuL here emphasizes its differences from previous concepts of a residual or intermediate layer. Since the BuL is intermittently turbulent, it can entrain fluid from both the underlying BL and the overlying FT (Russell et al., 1998). Therefore, Eq. (2) can be rewritten to assess the observed AOD:

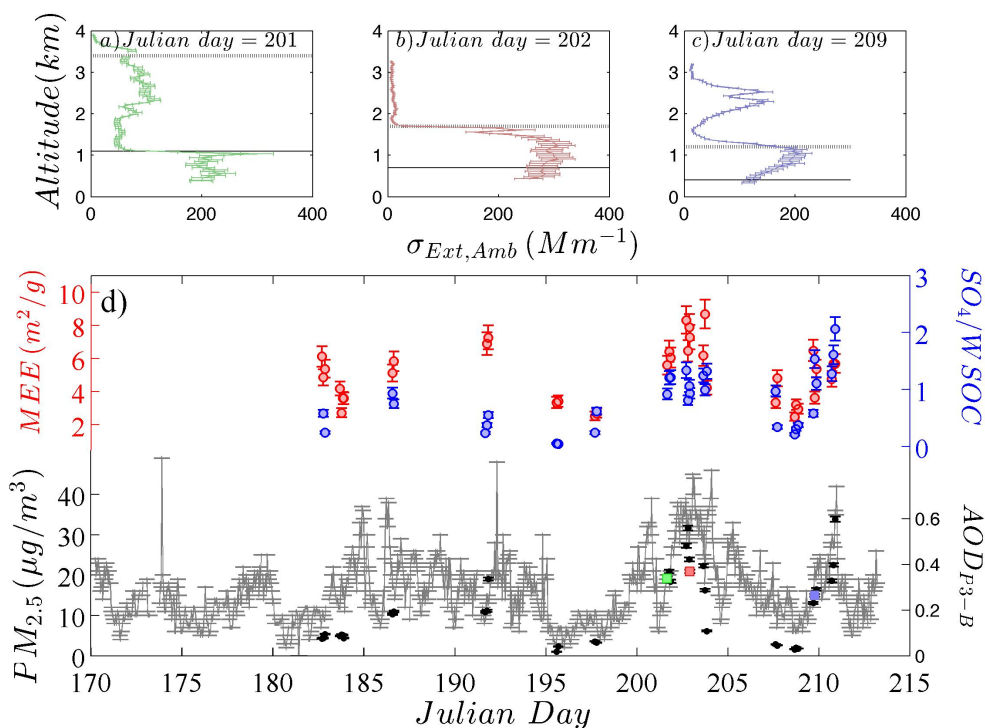


Fig. 4. Profiles (a, b, c) of the ambient extinction coefficient (550 nm) observed aboard the P-3B over Edgewood on 20, 21 and 28 July 2011, respectively. Time series (d) of the aerosol optical depth (AOD at 550 nm, black dots) calculated from the integration over the column of the extinction coefficients measured aboard the P-3B, the $PM_{2.5}$ measured from the Edgewood ground site (grey line), the mass extinction efficiency (MEE, red dots) and the ratio of the sulphate mass concentration over the water soluble organic mass concentration (blue dots) measured at the lowest level of the P-3B profiles.

Table 1. Aerosol optical depth (550 nm) calculated for the cases study shown in Fig. 4a, b, c for the boundary layer (BL), the buffer layer (BuL) and the free troposphere above the BuL (FT). The AOD contributions are indicated in the parentheses.

	Case 1 (Fig. 4 a)	Case 2 (Fig. 4b)	Case 3 (Fig. 4c)
Occurrence percentage	60	23	17
AOD _{BL}	0.23 (62 %)	0.17 (46 %)	0.05 (16 %)
AOD _{BuL}	0.14 (38 %)	0.18 (48 %)	0.14 (47 %)
AOD _{FT}	0.00 (0 %)	0.02 (5 %)	0.11 (37 %)

$$AOD = \int_{z_{surf}}^{z_{BL}} \sigma_{ext,amb}(z) dz + \int_{z_{BL}}^{z_{BuL}} \sigma_{ext,mb}(z) dz + \int_{z_{BuL}}^{z_{P3B}} \sigma_{ext,amb}(z) dz, \quad (4)$$

where z_{BL} , z_{BuL} , and z_{P-3B} denote the atmospheric boundary layer (BL) height, buffer layer (BuL) top, and the top of the P-3B sampling height, respectively. Each integral in Eq. (3) reflects the variation of the observed $\sigma_{ext,amb}$ (550 nm) as a function of the altitude, which is shown in Fig. 4a, b, c. These case studies, performed on 20 July 2011 (a), 21 July 2011 (b) and on 28 July 2011 (c), represent the three vertical aerosol distributions commonly observed during the campaign. The first case study on 20 July 2011 (Fig. 4a) represents more than 60 % of observations and highlights high values of $\sigma_{ext,amb}$ within the BL. The second study case on

21 July 2011 (Fig. 4b) represents 17 % of the observed profiles and shows the presence of the aerosol capped by the top of the BuL. Finally, an aerosol layer with significant $\sigma_{ext,amb}$ values (550 nm) can be detected above the buffer layer (case on 28 July 2011, Fig. 4c). Table 1 describes the averaged contribution of the aerosols present within each layer to the total AOD_{550 nm} for the three different vertical aerosol distributions observed during DISCOVER-AQ. The presence of an aerosol layer aloft the BL, accounting for a large part of the AOD_{550 nm}, has been observed in 40 % of the profiles. One can see that the BuL contribution to the total AOD is on average larger than 38 % and is thus nonnegligible. Moreover, when an aerosol layer is present aloft the BuL, the averaged contribution of the aerosol within the BL to the total AOD_{550 nm} decreases to 16 %.

$\sigma_{\text{ext,dry}}(z)$ can be expressed as the product of the mass extinction efficiency (MEE_{dry}) and aerosol mass loading (M_{dry}):

$$\sigma_{\text{ext,dry}} = \text{MEE}_{\text{dry}} \cdot M_{\text{dry}}. \quad (5)$$

Furthermore, the value of $\sigma_{\text{ext,dry}}$ has a variability of 9% within the BL based on BL averages for all profiles. Thus, it is reasonable to believe that the BL is vertically well mixed and, assuming that aerosol loading above the BL is negligible, Eq. (3) can be further reduced to Eq. (6), which is commonly cited in the literature (e.g., Koelemeijer et al., 2006):

$$\text{PM}_{2.5} = \frac{f \text{RH}_{\text{amb}} \text{MEE}_{\text{dry,surf}} z_{\text{BL}}}{\text{AOD}} \quad (6)$$

The large number of profiles acquired during the DISCOVER-AQ campaign offers a unique opportunity to study the validity and the impact of the assumptions made in Eq. (6).

5 Results

During the campaign, the PM_{2.5} observations performed at each of the three relevant ground sites show similar temporal tendencies. A time series for PM_{2.5} at the Edgewood site is shown in Fig. 4d along with the AOD_{550 nm}, the derived mass extinction efficiency (MEE, 550 nm), and the sulfate-to-WSOC (water soluble organic carbon) as a function of the Julian day. This time series highlights the large range of the hourly averaged PM_{2.5} values within a highly polluted period (Julian day 201–205, PM_{2.5} greater than 30 $\mu\text{g m}^{-3}$) and a clean period (Julian day 195–199, PM_{2.5} less than 10 $\mu\text{g m}^{-3}$). Note the largest PM_{2.5} values are associated with the highest sulfate/WSOC ratio and the largest effective radius (calculated as the ratio of 3rd and 2nd moments of the UHSAS aerosol size distribution, Fig. 5). In order to determine the geographical origins and the history of these air masses, back trajectory calculations are performed using the HYSPLIT (Hybrid Single Particle Lagrangian Integrated Trajectory) model (Draxler and Rolph, 2010). HYSPLIT was initialized for each ground site for every P-3B profile four days backward in time. During clean periods, the back trajectories did not show any systematic pattern for the air mass origins, while highly polluted periods were associated with air masses coming from the Ohio River valley, a region typically associated with power plant emissions. Indeed, Peltier et al. (2007) reported sulfate concentration up to 30 $\mu\text{g m}^{-3}$ over this region during the New England Air Quality Study (NEAQS) airborne field campaign in 2002, and Ziemba et al. (2007) found enhanced ammonium sulfate concentrations associated with long-range transport events from this region to the northeast United States during ICARTT in 2004. The differences in the aerosol sources may also explain the effective radius differences, as emissions of primary organic

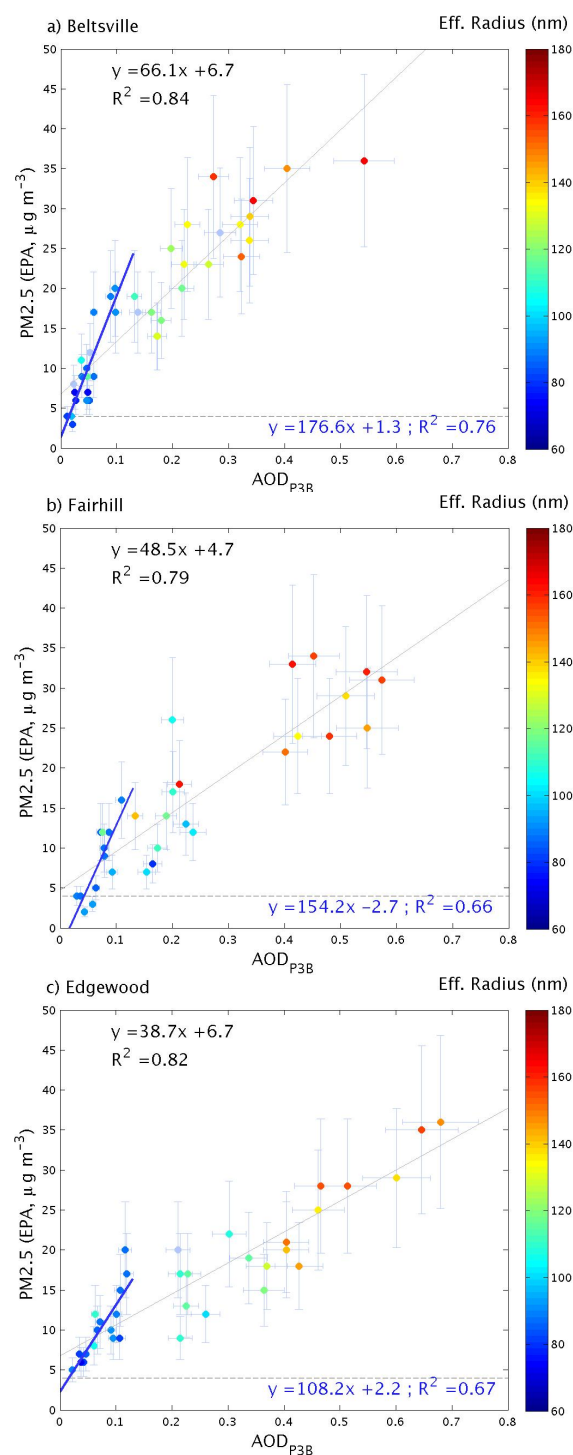


Fig. 5. PM_{2.5} measured from the EPA ground sites (at Beltsville (a), Fairhill (b), and Edgewood (c)) as a function of the AOD (550 nm) calculated using extinction profiles performed by the P-3B. The color code represents the effective radius (nm). The horizontal dashed line corresponds to the detection limit of the BAM (4 $\mu\text{g m}^{-3}$). The error bars correspond to the measurement variability ($\pm 1\sigma$). The grey fit (equation in black) is for all retrieved AOD values, while the blue fit is for cases with prevalent fine-mode aerosols ($R_{\text{eff}} < 100$ nm).

aerosol are typically of smaller diameter (Zhang et al., 2005; Volkamer et al., 2006).

The aerosol chemical composition is strongly linked with the aerosol size distribution, with larger particles being enriched with sulfate. The aerosol MEE_{550 nm}, sensitive to both aerosol physical and chemical properties, was calculated using the PM_{2.5} and the average dry aerosol extinction (550 nm) measured at the lowest P-3B flight altitude. The MEE_{550 nm} varied between 2.6 and 9.7 m² g⁻¹ during the entire campaign with a median of 5.04 m² g⁻¹. The highest MEE_{550 nm} values correspond to PM_{2.5} values close to the detection limit (<4 μg m⁻³). By filtering the MEE_{550 nm} as a function of the sulfate concentration, two distinct aerosol MEEs were observed during the DISCOVER-AQ campaign: aerosols enriched in sulfate related to power plant emissions (MEE_{550 nm} ~5.3 ± 0.4 m² g⁻¹) and aerosols enriched in organics related to urban emission (MEE_{550 nm} ~3.8 ± 0.9 m² g⁻¹). These values are consistent with previous studies. Husar et al. (2000) reported MEE values measured on the east coast of the United States, on average about 4.9 m² g⁻¹. Moreover, Pereira et al. (2008) measured the MEE values of anthropogenic pollution present over Portugal in 2006 and observed values around 3 m² g⁻¹, while Horvath et al. (1992) measured the MEE of ammonium sulfate, (NH₄)₂SO₄, to be 6 m² g⁻¹.

Figure 5 shows the correlation between PM_{2.5} measured from the EPA ground sites at (a) Beltsville, (b) Fairhill, and (c) Edgewood and the AOD_{550 nm} calculated for each profile performed by the P-3B. The color code corresponds to the effective radius. As previously stated, the profiles performed over Beltsville were confined to altitudes lower than 1.5 km (due to air traffic controller restrictions) while those performed over Fairhill and Edgewood reached 3 km. The integration of the extinction coefficient over a different altitude range may have caused an underestimation of the AOD_{550 nm} over Beltsville. An orthogonal distance regression has been applied for each site for all data (regardless of particle effective radius) and is displayed in the top left corner of each figure. Correlations between integrated column and surface measurements are very strong (correlation coefficients larger than 0.84 at Beltsville, 0.79 at Fairhill and 0.82 at Edgewood). The slopes are similar for each site, 66.1 (μg m³ per unit of AOD_{550 nm}) at Beltsville, 48.5 at Fairhill, and 38.7 at Edgewood. Hoff and Christopher (2009) summarized the linear regressions between the AOD_{550 nm} and the PM_{2.5} obtained over the United States, Europe and China from 15 independent studies. They found the average slope, calculated using only the studies over the United States, was approximately 63 ± 51. Moreover, Engel-Cox et al. (2006) retrieved a slope between 31 and 49 over Baltimore during the summer 2004, which is in good agreement with the values obtained in this study.

Hoff and Christopher (2009) discussed a hypothetical non-linearity between AOD and PM_{2.5} based on simulation results (Liu et al., 2005) and assumed that this hypothetical

Table 2. The lower 10th, median and 90th percentile of the boundary layer and the buffer layer (when it exists) contributions to the total AOD (%). The sample number is given under “N”.

Ground site	Boundary Layer (BL)			Buffer Layer (BuL)				
	N	10th	Med	90th	N	10th	Med	90th
Beltsville *	–	–	–	–	–	–	–	–
Fairhill	29	42	61	80	25	11	27	42
Edgewood	32	36	57	78	29	12	32	51

* The profiles performed over Beltsville were limited by the air traffic controllers to a maximum altitude of 1.5 km, which may have caused an underestimation of the AOD_{550 nm} and limited the exploration of the BuL.

nonlinearity would be due to a sparse distribution of the AOD values during clean periods (especially for AOD < 0.1). As more than 40 % of the P-3B profiles were performed during clean periods, DISCOVER-AQ offers a great opportunity to study this nonlinearity. According to Fig. 5, these clean periods are related to the presence of small particles (75 < R_{eff} < 100 nm) enriched in organics (MEE_{550 nm} ~4 m² g⁻¹) in contrast to polluted periods dominated by larger (R_{eff} greater than 100 nm) sulfate particles. According to Mie theory, small particles (R_{eff} less than 100 nm) are significantly less optically active than larger particles, but still impact the total aerosol mass. Therefore, the presence of small particles induces nonlinearity between the AOD_{550 nm} and the PM_{2.5}, which is clearly depicted by the linear fits (blue lines) using exclusively the clean periods shown in Fig. 5 for each site. The slopes differ by a factor between 2.5 and 3 and highlight the low extinction efficiency of the small particles (75 < R_{eff} < 100 nm); values of 177, 154, 108 μg m³ per unit of AOD_{550 nm} were derived for Beltsville, Fairhill, and Edgewood, respectively. Therefore, these results show the necessity of measurements at multiple wavelengths, i.e., determination of the Ångström Exponent, to account for the nonlinearities in the PM_{2.5}-AOD_{550 nm} relationship due to the presence of small particles. The effective radius and the Ångström exponent measured aboard the P-3B are found to be directly related (see the Supplement). The lower values of the Ångström Exponent are associated to the larger particles while the larger values (> 2.3) are related to the presence of small particles (< 100 nm). Thus, the nonlinearities, during this campaign, can be avoided using a threshold value for the Ångström exponent (around 2.3, see Fig. 1 in the Supplement).

5.1 Factors affecting the relationship between AOD and PM_{2.5}

5.1.1 Aerosol vertical distribution

Using the meteorological parameters measured during the P-3B profiles, the top of the BL ranged from 500 to 2200 m, with the minimum height generally observed during the morning and gradually increasing during the day, consistent with the increase in heating in the lower troposphere. From

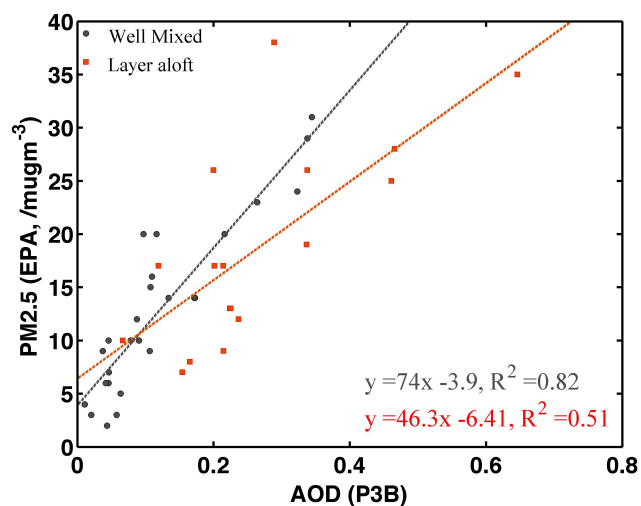


Fig. 6. PM_{2.5} measured from the EPA ground sites (Beltsville, Edgewood and Fairhill) as a function of the AOD_{550 nm} calculated using extinction profiles performed by the P-3B when an elevated aerosol layer aloft the BL was observed (red squares) or absent (black dots).

the BL structure analyses (D. Lenschow, personal communication, 2013) for the DISCOVER-AQ project, a distinct BuL was present in 80 % of the profiles (192 of 240). Overall, the AOD_{550 nm} contribution from the BL was between 57–61 % (Table 2). Considering the study cases presented in Fig. 4, the BL contribution to the AOD_{550 nm} in the usual case (i.e., highly concentrated BL and no aerosol layer aloft similar to 20 July 2011) is about 60 %, while the BuL contribution is lower than 27 %. The presence of an aerosol layer aloft (i.e., similar to 21 or 28 July 2011) dramatically decreases the BL contribution to the AOD_{550 nm} (less than 37 %), and thus the extinction from aerosols present in the BuL dominates the AOD_{550 nm} (contribution of approximately 60 %). By sorting the data as a function of the presence or the absence of a layer aloft the BL, two distinct tendencies can be observed (Fig. 6). Indeed, when the aerosols are confined in the BL, the correlation coefficient between AOD_{550 nm} and the PM_{2.5} is relatively high (0.91) and the slope is approximately 74, while the presence of an elevated layer leads to a wider spread of the data set ($R^2 = 0.71$) and a lower slope (46.3). Thus, the presence of this layer may lead to an underestimation by a factor of 1.6 of the PM_{2.5} at the surface. These results illustrate the potential pitfall of PM_{2.5} estimation when lofted layers are present.

Figure 7 shows comparisons between AOD_{550 nm} derived from the P-3B profiles, the ground-based aerosol mass (PM_{2.5}), and aerosol volume measured at the lowest P-3B flight level scaled by $f(\text{RH})_{\text{amb}}$ and the height of the surface-coupled, mixed layer. The BL and the BuL heights (bounding the height of the layer (including the BL and the BuL) in which most of the aerosols are observed) are used to represent the height of this mixed layer. The color code represents

the BL (Fig. 7a, b) and the BL + BuL (Fig. 7c, d) contribution to the total AOD_{550 nm} and highlights the importance of that parameter to retrieve the air quality from the AOD. The PM_{2.5} measurements were limited to 3 out of the 6 ground sites, while the aerosol volume was measured aboard the P-3B over the 6 ground sites and thus offers a more statistically robust comparison (Fig. 7b, d). Moreover, the comparison of the PM_{2.5} with the aerosol volume concentration measured at the lowest level of the P-3B profiles shows high correlation coefficients (0.93, 0.92 and 0.89 respectively at Beltsville, Fairhill, and Edgewood).

He et al. (2008) have shown that the haze layer concept (the haze layer top is defined by the height where the aerosol extinction coefficient decreases to 1/e times the aerosol extinction coefficient at the top of the BL) improves the relationship between PM_{2.5} and the AOD. By integrating Eq. (2) from the surface to the top of the BuL (available from radio soundings), the relationship between the AOD_{550 nm} and the PM_{2.5} is strongly improved (Fig. 7c, d, $R^2 > 0.95$ compare to $R^2 \sim 0.84$ using the BL). The same study has been done using the haze layer calculated from the HSRL measurements (Scarino et al., 2013), showing similar improvements ($R^2 > 0.95$). Nevertheless, the haze layer is a Lidar product and might not be available for most studies trying to assess the AOD and PM_{2.5} relationship. The strong relationships (with low variability) between column integrated measurements and the averaged volume of the aerosols sampled within the BL + BuL show that using the BuL height instead of the BL height, provided by radiosounding measurements, will improve the PM_{2.5} retrievals from the AOD_{550 nm}.

While we show that using the BuL height as the aerosol layer top is reasonable for the large observational data set obtained in the Baltimore–Washington metropolitan area, there may be other locations where this assumption does not hold. Indeed, the systematic presence of an aerosol layer above the BuL (only 17 % of the profiles in this study, Fig. 4c) would increase the variability of the correlation shown in Fig. 7d. Thus, this study motivates additional work focusing on the relationship between AOD and PM_{2.5} in environments where aerosol layers are frequently observed above the well-defined BL and BuL (e.g., African coast, SE United States) or in regions with especially shallow BL or BuL heights (e.g., wintertime San Joaquin Valley, CA, USA).

The direct comparison of the calculated AOD (550 nm, Fig. 5) and the measured PM_{2.5} shows a strong correlation without taking into account the BL height and $f(\text{RH})$ constraints most likely due to similar properties of the aerosol sampled within the BL and the BuL (e.g., $f(\text{RH}) = 80\%$ and effective radius). Figure 8 shows a comparison of BL and BuL values for effective radius and $f(\text{RH}) = 80\%$. The plots show the parameter averages for each vertical layer (BL or BuL) during each P-3B profile and highlight the strong similarities of the aerosol physical (represented by effective radius) and chemical (represented by $f(\text{RH}) = 80\%$) properties in each layer. Indeed, more than 76 % of the

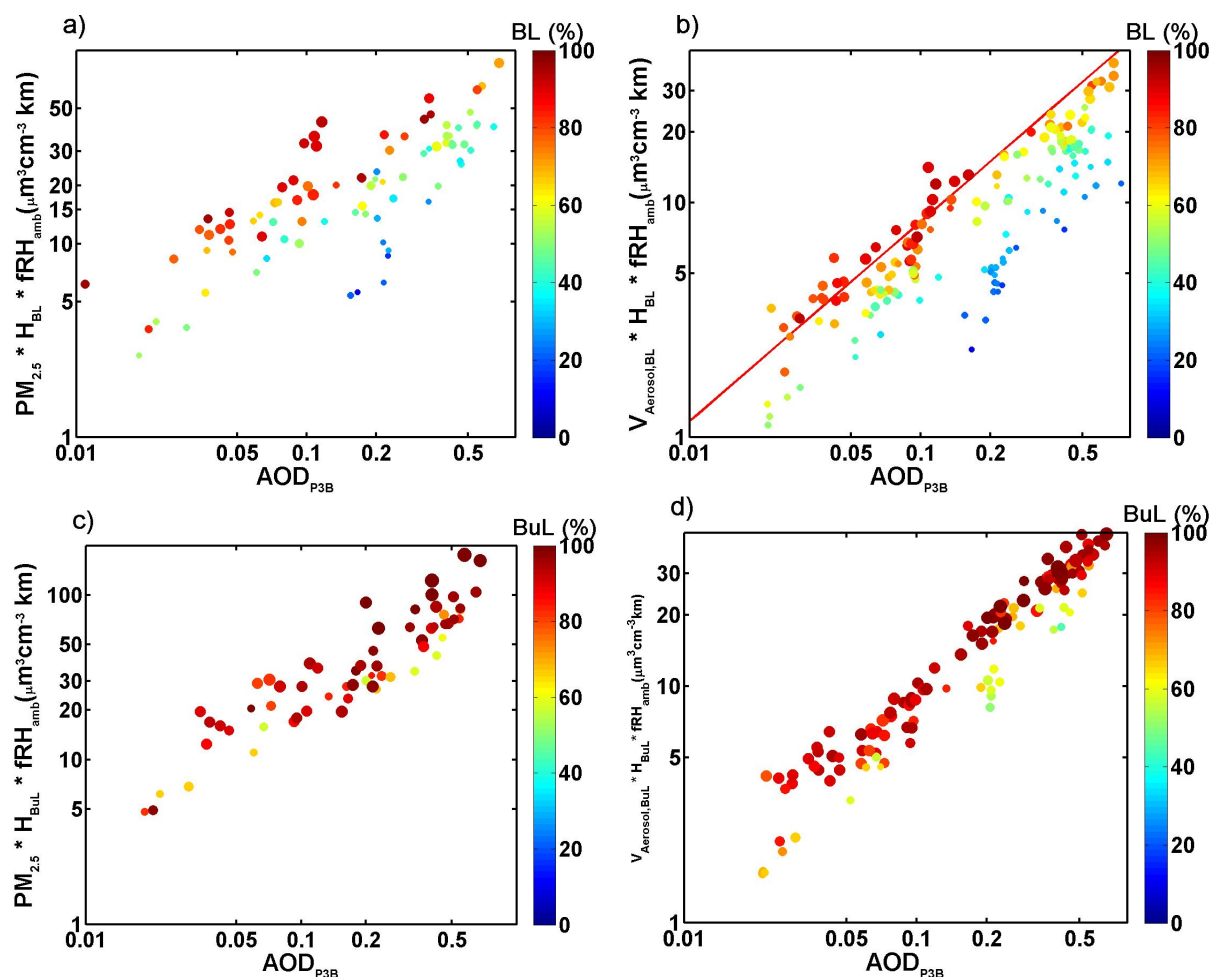


Fig. 7. PM_{2.5} values weighted by varying factors as a function of the ambient AOD_{550 nm} measured by the P-3B. **(a)** uses the BL height and $f(\text{RH})_{\text{amb}}$, **(b)** uses the BL height and volume concentrations measured aboard the P-3B, **(c)** uses the BuL height and $f(\text{RH})_{\text{amb}}$, and **(d)** uses the BuL height and volume concentrations. The color code represents the BL (BL + BuL) contribution to the AOD and the size of each dot correspond to the BL (BuL) height ((a), (b) and (c), (d) respectively). The red line is corresponding to the linear fit of cases where the AOD contribution of the BL is higher than 75 %.

effective radius and 88 % of the $f(\text{RH}=80\%)$ values are within $\pm 10\%$ of the 1 : 1 line. Very few cases during this campaign show important differences in the aerosol physical or chemical properties. Differences between the BL and BuL aerosol properties might be more frequent over some regions where the atmospheric vertical structure of aerosols is strongly influenced by different aerosol sources.

5.1.2 Relative humidity

High relative humidity conditions, frequently encountered in the BL and in the vicinity of clouds, can result in significant modifications of the optical properties (Hänel, 1984; Twohy et al., 2009; Schuster et al., 2009) due to aerosol hydration. To account for this effect, the frequency of the AOD_{550 nm} (calculated from the $\sigma_{\text{ext,amb}}$ measured at 550 nm aboard the P-3B or measured by AERONET) at ambient relative humid-

ity as well as water fraction (WF) (Eq. 7, Shinzuka et al., 2007) are analyzed (Fig. 9):

$$\text{WF} = 1 - \frac{\text{AOD}_{\text{dry}}}{\text{AOD}_{\text{amb}}} \quad (7)$$

For most cases (>60 %), the AOD_{550 nm} values measured at ambient RH during this campaign were lower than 0.2. Several studies report AOD_{550 nm} reference values for remote (Mauna Loa, Hawaii; Holben et al., 2001), rural (Lamont (Oklahoma), Andrews et al., 2011; Bondsville (Illinois), Fort Peck (Montana), Goodwin Creek (Mississippi), Table Mountain (Colorado), Penn State (Pennsylvania) and Sioux Falls (South Dakota) Augustine et al., 2008) and urban (Goddard Space Flight Center [GSFC], Maryland; Holben et al., 2001) USA regions. All AOD_{550 nm} observed in the remote atmosphere are below 0.06 all year long (for about 5 years of measurements), over rural areas their values vary

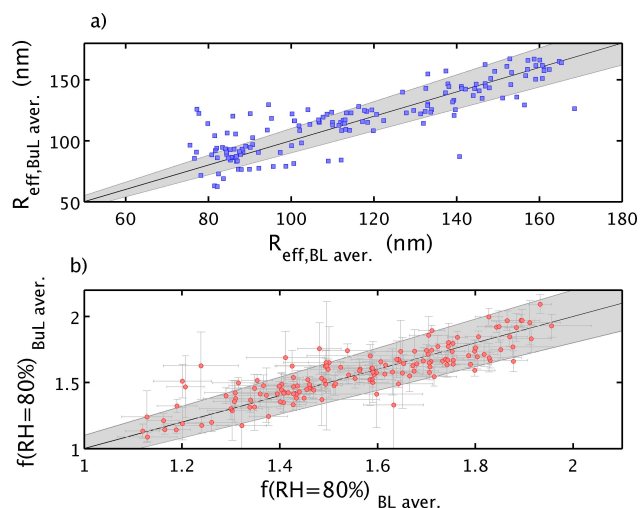


Fig. 8. Comparison of the effective radius (a) and $f(\text{RH}=80)_{550 \text{ nm}}$ (b) averaged within the BL (boundary layer) and the BuL (buffer layer) for all the DISCOVER-AQ sites (Beltsville, Padonia, Fairhill, Aldino, Edgewood and Essex). The black line corresponds to the 1 : 1 line and the gray area represents the 10 % variability.

between 0.11 and 0.47 during the summer period (using at least 3 yr of measurements), while at GSFC the values were on average 0.5 ± 0.25 for the summer period (using 7 yr of measurements, 1992–1999). The values observed over the Baltimore–Washington metropolitan area are unusually low during DISCOVER-AQ in summer 2011 and are more representative of rural environment. Comparing the dry and wet AOD_{550 nm} highlights the contribution of the aerosol loadings versus the combined contribution of aerosol loading and water uptake. Lower AOD values (less than 0.1) were typically observed in conjunction with low RH (less than 50 %) and were not considered for this analysis. For all other cases, increased water fraction resulted in increased AOD: 15 % for AOD of 0.1, 35 % for AOD of 0.35. These results suggest that, at this location and for these profiles, the larger AOD values (>0.4) are mainly driven by water uptake.

During this campaign, the $f(\text{RH}=80)$ values, calculated at 550 nm, were observed to vary significantly from 1.28 to 1.91 on a day-to-day basis (Ziemba et al., 2013), but the profiles were fairly constant within the BL. The $f(\text{RH})_{\text{amb}}$ varied from 1.03 to 2.03 on a day-to-day basis. To isolate the dependence of AOD_{550 nm} on aerosol liquid water content effect from the aerosol vertical distribution, only the cases showing a BL contribution to the AOD_{550 nm} larger than 60 % were taken into account. Figure 10 shows the aerosol volume present in the BL (RH < 50 %), sorted as a function of the $f(\text{RH})_{\text{amb}}$ averaged in the BL (larger than 1.5 and lower than 1.2) as a function of the AOD_{P-3B}, calculated at ambient RH. It is interesting to note that the larger aerosol volume concentrations are associated to the larger values of the $f(\text{RH})_{\text{amb}}$. Slopes for the low $f(\text{RH})_{\text{amb}}$ values

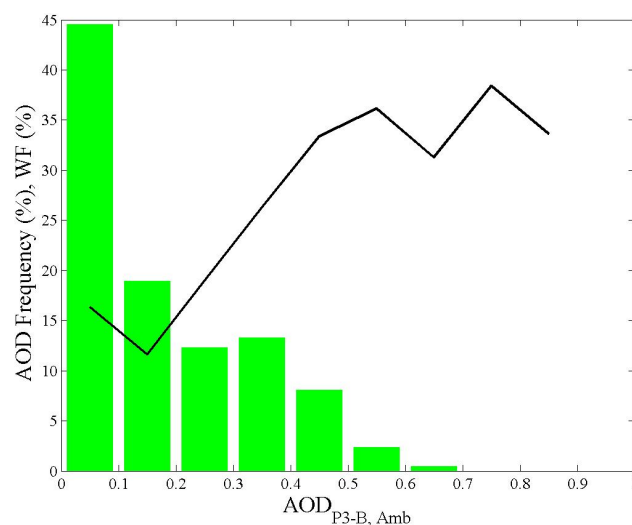


Fig. 9. Frequency of the AOD_{550 nm} retrieved from ambient extinction coefficient measured aboard the P-3B and the water fraction (WF in percent, black line) calculated using the dry and ambient AOD_{550 nm} measured aboard the P-3B (see Eq. 7).

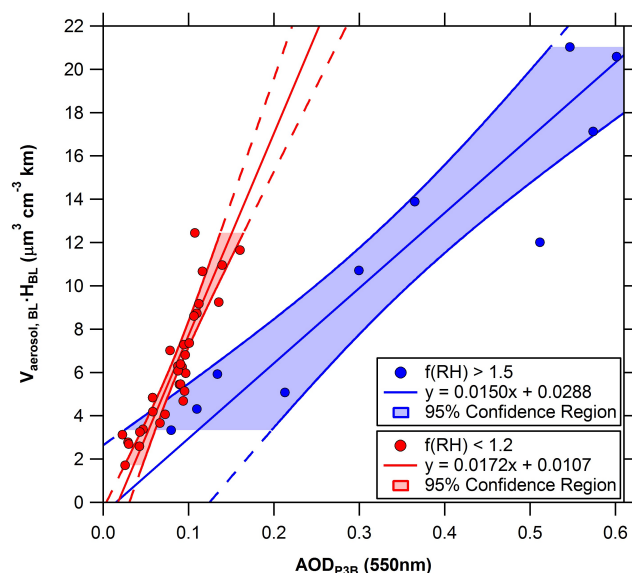


Fig. 10. Aerosol volume concentration averaged in the BL weighted by the BL height, when the aerosols present in the BL are contributing at 60 % and more, as a function of the AOD_{550 nm} from the P-3B measurements. The colors correspond to $f(\text{RH})_{\text{amb}, 550 \text{ nm}}$ values lower than 1.2 (red) and larger than 1.5 (blue).

are twice as high as those for the higher $f(\text{RH})_{\text{amb}}$ values (84 versus 40). PM_{2.5} retrievals for AOD_{550 nm} between 0.1 and 0.16 may vary from $6 \mu\text{m}^3 \text{cm}^{-3} \text{km}$ for aerosols associated with low $f(\text{RH})_{\text{amb}}$ values (<1.2) to $12 \mu\text{m}^3 \text{cm}^{-3} \text{km}$ for aerosols associated with high $f(\text{RH})_{\text{amb}}$ values (>1.5). The PM_{2.5} retrievals from AOD_{550 nm} measurements are thus highly dependent on the $f(\text{RH})_{\text{amb}}$ of the aerosols when the

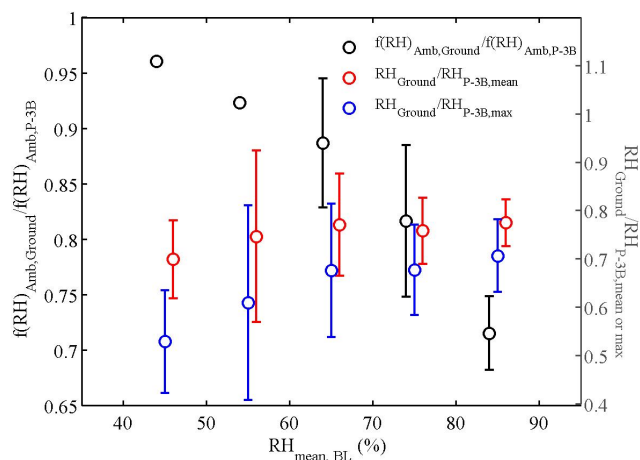


Fig. 11. Ratio of the $f(\text{RH})_{\text{amb,ground}}$ to $f(\text{RH})_{\text{amb,P-3B}}$ (black dots), of the averaged and maximum values as a function of the averaged relative humidity measured during the P-3B profiles within the BL.

measurements were performed. Ignoring or using an unsuitable $f(\text{RH})_{\text{amb}}$ of the aerosols could lead to a large error factor (from 1 up to 2, according to this data set) on the PM_{2.5} retrievals.

While $f(\text{RH})_{\text{amb}}$ vertical profiles are not yet available on a global scale, ground measurements of $f(\text{RH})_{\text{amb}}$ or RH are available and can be applied to the entire column to improve the estimation of PM_{2.5} from the AOD_{550 nm}. To estimate the errors induced by using the ground measurements, the $f(\text{RH})_{\text{amb,ground}}$ was calculated using the RH measured at the ground sites and the scattering coefficients (ambient and dry at 550 nm) measured at the lowest level of the P-3B profiles (Fig. 11). Under dry conditions, reasonable agreement (< 10 % error) is observed between the ground-based and P-3B $f(\text{RH})_{\text{amb}}$ measurements; however, this agreement worsens considerably at RH > 75 % (errors larger than 19 %). Therefore, in order to estimate the PM_{2.5} from the AOD_{550 nm}, the ground $f(\text{RH})_{\text{amb}}$ measurements should be used only when the relative humidity throughout the atmospheric column is lower than 55 %.

Similarly, the average and maximum values of the relative humidity measured aboard the P-3B are compared to the relative humidity measured at the ground. Ground-level extrapolation through the column always results in an underestimation of true RH, by 50 % under dry BL conditions and 30 % under wet BL conditions.

6 Conclusion

Over 240 profiles of aerosol optical, chemical, and microphysical properties were performed during the NASA DISCOVER-AQ, over the US Baltimore–Washington metropolitan area, offering an excellent opportunity to study the correlation between the air quality observations

at the surface and the column integrated measurements. The aerosol optical depth (AOD) was calculated using the integration of the extinction coefficient measured at 550 nm on board the P-3B throughout the column. The measurements were performed during one month and show that the aerosol mass concentrations (PM_{2.5}) measured at the surface (EPA ground sites) and the AOD time series show strong similarities. Sorting the AOD values with the water fraction highlights that the larger AOD values are driven by water fraction.

Three different atmospheric vertical structures were commonly observed: (i) the aerosol layer is capped by the boundary layer height (60 % of the profiles), (ii) an aerosol layer capped by the top of the BuL including the BL (23 % of the profiles), and (iii) an aerosol layer disconnected from the BuL and BL (17 % of the profiles). Previous studies (Al-Saadi et al., 2008; Tsai et al., 2011) have discussed the importance of taking into account the aerosol layer height to estimate more precisely the PM_{2.5} from the AOD. The observations show that the variability of the extinction coefficients within the boundary layer (BL) is low (< 9 %), allowing the linear integration over the entire BL altitude range. The contribution of the aerosol present within the BL to the total AOD is used to constrain the relationship between the AOD_{550 nm} and PM_{2.5}. As a result, different AOD versus PM_{2.5} slopes are observed as a function of the presence and the optical thickness of the elevated aerosol layer. Thus, the height of the BL layer combined with the BL contribution improves the PM_{2.5} estimation from AOD_{550 nm}. Using the top of the BuL instead of the BL top as the height for the aerosol layer dramatically improves the PM_{2.5} estimation.

During this campaign, the $f(\text{RH})_{\text{amb}}$ effect on the estimation of the PM_{2.5} is found to be secondary compared to the aerosol vertical distribution and the contribution of the aerosol within the BL, and induced an error factor varying from 1 to 2. Moreover, the comparison of the observed $f(\text{RH})_{\text{amb,P-3B}}$ and the calculated $f(\text{RH})_{\text{amb,ground}}$ shows that the errors are lower than 10 % when the BL is relatively dry (< 55 %), while the errors are larger than 19 % when the BL is relatively humid (larger than 75 %).

This work examines the uncertainties associated with the use of AOD measurements to estimate ground-based PM_{2.5}, and finds that accurate quantification of the aerosol mixed-layer height is paramount for accurately predicting PM_{2.5} concentrations, while capturing the compositional-based $f(\text{RH})_{\text{amb}}$ variability is less important for PM_{2.5} estimation. During clear sky conditions, the $f(\text{RH})_{\text{amb}}$ variability is found to be a second-order effect in the overall estimates. Since these results are representative of the Baltimore–Washington metropolitan area, extrapolating these results to other geographical locations must be done with care. The four field campaigns planned during the DISCOVER-AQ project offer an opportunity to perform similar studies over different regions characterized by a wide variety of aerosol sources and meteorological conditions. Together

these studies will provide a better understanding of the ability of future remote-sensing retrievals to quantify surface PM_{2.5} on a global or regional scale.

Supplementary material related to this article is available online at <http://www.atmos-chem-phys.net/14/2139/2014/acp-14-2139-2014-supplement.pdf>.

Acknowledgements. This research was funded by NASA's Earth Venture-1 Program through the Earth System Science Pathfinder Program Office. The authors wish to thank the ESSP Program Office for their support throughout the first DISCOVER-AQ deployment. We would also like to express our deep appreciation to Mary Kleb as well as the pilots and flight crews of NASA's P-3B and UC-12 for their important contributions. We thank B. Holben (NASA-GSFC) for providing the Sun photometer within the framework of the AERONET program. Finally, we would like to thank the Maryland Department of Environment and EPA for making the PM_{2.5} and the ozone measurements available and sharing their data with DISCOVER-AQ. Suzanne Crumeyrolle and Richard H. Moore have been supported by the NASA Postdoctoral Program fellowship.

Edited by: N. Riemer

References

- Al-Saadi, J., Soja, A., Pierce, R. B., Szykman, J., Wiedinmyer, C., Emmons, L., Kondragunta, S., Zhang, X., Kittaka, C., Schaack, T., and Bowman, K.: Intercomparison of near-real-time biomass burning emissions estimates constrained by satellite fire data, *J. Appl. Remote Sens.*, 2, 021504, doi:10.1117/1.2948785, 2008.
- Anderson, T. L. and Ogren, J. A.: Determining aerosol radiative properties using the TSI 3563 integrating nephelometer, *Aerosol Sci. Technol.*, 29, 57–69, 1998.
- Andrews, E., Sheridan, P. J., Ogren, J. A., and Ferrare, R.: In Situ Aerosol Profiles over the Southern Great Plains CART site, Part I: Aerosol Optical Properties, *J. Geophys. Res.*, 109, D06208, doi:10.1029/2003JD004025, 2004.
- Andrews, E., Sheridan, P. J., and Ogren, J. A.: Seasonal differences in the vertical profiles of aerosol optical properties over rural Oklahoma, *Atmos. Chem. Phys.*, 11, 10661–10676, doi:10.5194/acp-11-10661-2011, 2011.
- Annesi-Maesano, I., Forastiere, F., Kunzli, N., and Brunekref, B.: Particulate matter, science and EU policy, *Europ. Respirat. J.*, 29, 428–431, 2007.
- Augustine, J. A., Hodges, G. B., Dutton, E. G., Michalsky, J. J., and Cornwall, C. R.: An aerosol optical depth climatology for NOAA's national surface radiation budget network (SURFRAD), *J. Geophys. Res.*, 113, D11204, doi:10.1029/2007JD009504, 2008.
- Beyersdorf A. J., Chen, G., Crumeyrolle, S., Thornhill, K. L., Winstead, E., Ziemba, L. D., and Anderson, B. E.: Aerosol Composition and Variability in the Baltimore-Washington D.C. Region, in preparation for *Atmos. Chem. Phys. Discuss.*, 2014.
- Carrico, C. M., Rood, M. J., and Ogren, J. A.: Aerosol light scattering properties at Cape Grim, Tasmania, during the First Aerosol Characterization Experiment, *J. Geophys. Res.*, 103, 16565–16574, 1998.
- Carrico, C. M., Rood, M. J., and Ogren, J. A.: Aerosol light scattering properties at Sagres, Portugal, during ACE-2, *Tellus 52B*, 694–715, 2000.
- Chu, D. A., Kaufman, Y. J., Zibordi, G., Chern, J. D., Mao, J., Li, C., and Holben, B. N.: Global monitoring of air pollution over land from the Earth Observing System-Terra Moderate Resolution Imaging Spectroradiometer (MODIS), *J. Geophys. Res.*, 108, 4661, doi:10.1029/2002JD003179, 2003.
- Collaud Coen, M., Andrews, E., Asmi, A., Baltensperger, U., Bukowiecki, N., Day, D., Fiebig, M., Fjaeraa, A. M., Flentje, H., Hyvärinen, A., Jefferson, A., Jennings, S. G., Kouvarakis, G., Lihavainen, H., Lund Myhre, C., Malm, W. C., Mihapopoulos, N., Molenaar, J. V., O'Dowd, C., Ogren, J. A., Schichtel, B. A., Sheridan, P., Virkkula, A., Weingartner, E., Weller, R., and Laj, P.: Aerosol decadal trends – Part 1: In-situ optical measurements at GAW and IMPROVE stations, *Atmos. Chem. Phys.*, 13, 869–894, doi:10.5194/acp-13-869-2013, 2013.
- Day, D. E. and Malm, W. C.: Aerosol light scattering measurements as a function of relative humidity: A comparison between measurements made at three different sites, *Atmos. Environ.*, 35, 5169–5176, doi:10.1016/S1352-2310(01)00320-X, 2001.
- Draxler, R. R. and Rolph, G. D.: HYSPLIT (HYbrid Single-Particle Lagrangian Integrated Trajectory), Model access via NOAA ARL READY Website <http://ready.arl.noaa.gov/HYSPLIT.php>, NOAA Air Resources Laboratory, Silver Spring, MD, 2010.
- Engel-Cox, J. A., Holloman, C. H., Coutant, B. W., and Hoff, R. M.: Qualitative and quantitative evaluation of MODIS satellite sensor data for regional and urban scale air quality, *Atmos. Environ.*, 38, 2495–2509, doi:10.1016/j.atmosenv.2004.01.039, 2004.
- Engel-Cox, J. A., Hoff, R. M., Rogers, R., Dimmick, F., Rush, A. C., Szykman, J. J., Al-Saadi, J., Chu, D. A., and Zell, E. R.: Integrating LIDAR and satellite optical depth with ambient monitoring for 3-D dimensional particulate characterisation, *Atmos. Environ.*, 40, 8056–8067, 2006.
- Esteve, A. R., Ogren, J. A., Sheridan, P. J., Andrews, E., Holben, B. N., and Utrillas, M. P.: Sources of discrepancy between aerosol optical depth obtained from AERONET and in-situ aircraft profiles, *Atmos. Chem. Phys.*, 12, 2987–3003, doi:10.5194/acp-12-2987-2012, 2012.
- Fierz-Schmidhauser, R., Zieger, P., Wehrle, G., Jefferson, A., Ogren, J. A., Baltensperger, U., and Weingartner, E.: Measurement of relative humidity dependent light scattering of aerosols, *Atmos. Meas. Tech.*, 3, 39–50, doi:10.5194/amt-3-39-2010, 2010.
- Gao, R. S., Ballard, J., Watts, L. A., Thornberry, T. D., Ciciora, S. J., McLaughlin, R. J., and Fahey, D. W.: A compact, fast UV photometer for measurement of ozone from research aircraft, *Atmos. Meas. Tech.*, 5, 2201–2210, doi:10.5194/amt-5-2201-2012, 2012.
- Gassó, S., Hegg, D. A., Covert, D. S., Collins, D. R., Noone, K. J., Öström, E., Schmid, B., Russell, P. B., Livingston J. M., Durkee, P. A., and Jonsson, H. H.: Influence of humidity on the aerosol scattering coefficient and its effect on the upwelling radiance during ACE-2, *Tellus 52B*, 546–567, 2000.
- Gupta, P. and Christopher, S. A.: Particulate matter air quality assessment using integrated surface, satellite, and meteorological

- products: Multiple regression approach, *J. Geophys. Res.*, 114, D14205, doi:10.1029/2008JD011496, 2009a.
- Gupta, P. and Christopher, S. A.: Particulate matter air quality assessment using integrated surface, satellite, and meteorological products: 2. A neural network approach, *J. Geophys. Res.*, 114, D20205, doi:10.1029/2008JD011497, 2009b.
- Gupta, P., Christopher, S. A., Wang, J., Gehrig, R., Lee, Y., and Kumar, N.: Satellite remote sensing of particulate matter and air quality assessment over global cities. *Atmos. Environ.*, 40, 5880–5892, 2006.
- Gupta, P., Christopher, S. A., Box, M. A., and Box, G. P.: Multi year satellite remote sensing of particulate matter air quality over Sydney, Australia, *Int. J. Remote Sens.*, 28, 4483–4498, 2007.
- Hänel, G.: The properties of atmospheric aerosol particles as functions of the relative humidity at thermodynamic equilibrium with the surrounding moist air, *Adv. Geophys.*, 19, 74–189, 1976.
- Hänel, G.: Parameterization of the influence of relative humidity on optical aerosol properties, edited by: Gerber, H. and Deepak, A., in: *Aerosols and their climatic effects*, 117–122. A. Deepak, Hampton, VA, 1984.
- Hartley, W. S., Hobbs, P. V., Ross, J. L., Russell, P. B., and Livingston, J. M.: Properties of aerosols aloft relevant to direct radiative forcing off the mid-Atlantic coast of the United States, *J. Geophys. Res.*, 105, 9859–9885, 2000.
- He, Q., Li, C., Mao, J., Lau, A. K.-H., and Chu, D. A.: Analysis of aerosol vertical distribution and variability in Hong Kong, *J. Geophys. Res.*, 113, D14211, doi:10.1029/2008JD009778, 2008.
- Hegg, D., Larson, T., and Yuen, P.-F.: A theoretical study of the effect of relative humidity on light scattering by tropospheric aerosols, *J. Geophys. Res.*, 98, 18435–18439, 1993.
- Hoff, R. M. and Christopher, S. A.: Remote sensing of Particulate Pollution from Space: Have we reached the Promised Land?, *J. Air Waste Manage. Assoc.*, 59, 645–675, doi:10.3155/1047-3289.59.6.645, 2009.
- Holben, B. N., Eck, T. F., Slutsker, I., Tanré, D., Buis, J. P., Setzer, A., Vermote, E., Reagan, J. A., Kaufman, Y. J., Nakajima, T., Lavenue, F., Jankowiak, I., and Smirnov, A.: AERONET—A Federated Instrument Network and Data Archive for Aerosol Characterization, *Remote Sens. Environ.*, 66, 1–16, 1998.
- Holben, B. N., D. Tanre, A. Smirnov, T. F. Eck, I. Slutsker, N. Abuhassan, W. W. Newcomb, J. Schafer, B. Chatenet, F. Lavenue, Y. J. Kaufman, J. Vande Castle, A. Setzer, B. Markham, D. Clark, R. Frouin, R. Halthore, A. Karnieli, N. T. O'Neill, C. Pietras, R. T. Pinker, K. Voss, and G. Zibordi, An emerging ground-based aerosol climatology: Aerosol Optical Depth from AERONET, *J. Geophys. Res.*, 106, 12067–12097, 2001.
- Horvath, H.: Effects on visibility, weather and climate, edited by: Radojevic, M., Harrison, R. M., in: *Atmospheric Acidity. Sources, Consequences and Abatement*. Elsevier Applied Science, London, New York, pp. 435–466, 1992.
- Husar, R. B., Husar, J. D., and Martin, L.: Distribution of continental surface aerosol extinction based on visual range data, *Atmos. Environ.*, 34, 5067–5078, 2000.
- Kaufman, Y. J., Tanré, D., and Boucher, O.: A satellite view of aerosols in climate systems, *Nature*, 419, 215–223, 2002.
- Koelemeijer, R. B. A., Homan, C. D., and Matthijsen, J.: Comparison of spatial and temporal variations of aerosol optical thickness and particulate matter over Europe. *Atmos. Environ.*, 40, 5304–5315, 2006.
- Kumar, N., Chu, A., and Foster, A.: An empirical relationship between PM_{2.5} and aerosol optical depth in Delhi Metropolitan, *Atmos. Environ.*, 41, 4492–4503, 2007.
- Kumar, N., Chu, A., and Foster, A.: Remote sensing of ambient particles in Delhi and its environs: Estimation and validation, *Int. J. Remote Sens.*, 29, 3383–3405, 2008.
- Lenschow, D. H., Krumme, P. B., and Siems, S. T.: Measuring entrainment, divergence and vorticity on the mesoscale from an aircraft, *J. Atmos. Ocean. Technol.*, 16, 1384–1400, 1999.
- Liu, Y., Samat, J. A., Kilaru, V., Jacob, D. J., and Koutrakis, P.: Estimating Ground Level PM_{2.5} in the Eastern United States Using Satellite Remote Sensing, *Environ. Sci. Technol.*, 39, 3269–3278, 2005.
- Macias, E. S. and Husar, R. B.: Atmospheric particulate mass measurement with beta attenuation mass monitor, *Environ. Sci. Technol.*, 10, 904–907, 1976.
- McNaughton, C. S., Clarke, A. D., Howell, S. G., Pinkerton, M., Anderson, B. E., Thornhill, L., Hudgins, C., Winstead, E., Dibb, J. E., Scheuer, E., and Maring, H.: Results from the DC-8 Inlet Characterization Experiment (DICE): Airborne versus surface sampling of mineral dust and sea salt aerosols, *Aerosol Sci. Technol.*, 41, 136–159, doi:10.1080/02786820601118406, 2007.
- Peltier, R. E., Sullivan, A. P., Weber, R. J., Brock, C. A., Wollny, A. G., Holloway, J. S., de Gouw, J. A., and Warneke, C.: Fine aerosol bulk composition measured on WP-3D research aircraft in vicinity of the Northeastern United States – results from NEAQS, *Atmos. Chem. Phys.*, 7, 3231–3247, doi:10.5194/acp-7-3231-2007, 2007.
- Pereira, S., Wagner, F., and Silva, A. M.: Scattering properties and mass concentration of local and long range transported aerosols over the south western Iberian Peninsula, *Atmos. Environ.*, 42, 7623–7631, 2008.
- Pilinis, C. and Seinfeld, J.: Water content of atmospheric aerosols, *Atmos. Environ.*, 23, 1601–1606, 1989.
- Quinn, P. K., Bates, T. S., Baynard, T., Clarke, A. D., Onasch, T. B., Wang, W., Rood, M. J., Andrews, E., Allan, J., Carrico, C. M., Coffman, D., and Worsnop, D.: Impact of particulate organic matter on the relative humidity dependence of light scattering: A simplified parameterization, *Geophys. Res. Lett.*, 32, L22809, doi:10.1029/2005GL024322, 2005.
- Russell, L. M., Lenschow, D. H., Laursen, K. K., Krummel, P. B., Siems, S. T., Bandy, A. R., Thornton, D. C., and Bates, T. S.: Bidirectional mixing in an ace I marine boundary layer overlain by a second turbulent layer, *J. Geophys. Res.*, 103, 16411–16432, 1998.
- Ryder, C. L., Highwood, E. J., Rosenberg, P. D., Trembath, J., Brooke, J. K., Bart, M., Dean, A., Crosier, J., Dorsey, J., Brindley, H., Banks, J., Marsham, J. H., McQuaid, J. B., Sodemann, H., and Washington, R.: Optical properties of Saharan dust aerosol and contribution from the coarse mode as measured during the Fenec 2011 aircraft campaign, *Atmos. Chem. Phys.*, 13, 303–325, doi:10.5194/acp-13-303-2013, 2013.
- Scarino, A. J., Obland, M. D., Fast, J. D., Burton, S. P., Ferrare, R. A., Hostetler, C. A., Berg, L. K., Lefer, B., Haman, C., Hair, J. W., Rogers, R. R., Butler, C., Cook, A. L., and Harper, D. B.: Comparison of mixed layer heights from airborne high spectral resolution lidar, ground-based measurements, and the WRF-Chem model during CalNex and CARES, *Atmos.*

- Chem. Phys. Discuss., 13, 13721–13772, doi:10.5194/acpd-13-13721-2013, 2013.
- Schaap, M., Apituley, A., Timmermans, R. M. A., Koelemeijer, R. B. A., and de Leeuw, G.: Exploring the relation between aerosol optical depth and PM_{2.5} at Cabauw, the Netherlands, *Atmos. Chem. Phys.*, 9, 909–925, doi:10.5194/acp-9-909-2009, 2009.
- Schafer, K., Harbusch, A., Emeis, S., Koepke, P., and Wiegner, M.: Correlation of aerosol mass near the ground with aerosol optical depth during two seasons in Munich, *Atmos. Environ.*, 42, 4036–4046, 2008.
- Schmid, B., Livingston, J. M., Russell, P. B., Durkee, P. A., Jonsson, H. H., Collins, D. R., Flagan, R. C., Seinfeld, J. H., Gassó, S., Hegg, D. A., Öström, E., Noone, K. J., Welton, E. J., Voss, K. J., Gordon, H. R., Formenti, P., and Andreae, M. O.: Clear-sky closure studies of lower tropospheric aerosol and water vapor during ACE-2 using sunphotometer, airborne in-situ, spaceborne and ground-based measurements, *Tellus B*, 52, 568–593, 2000.
- Schmid, B., Flynn, C. J., Newsom, R. K., Turner, D. D., Ferrare, R. A., Clayton, M. F., Andrews, E., Ogren, J. A., Johnson, R. R., Russell, P. B., Gore, W. J., and Dominguez, R.: Validation of aerosol extinction and water vapor profiles from routine Atmospheric Radiation Measurement Climate Research Facility measurements, *J. Geophys. Res.*, 114, D22207, doi:10.1029/2009JD012682, 2009.
- Schuster, G. L., Lin, B., and Dubovik, O.: Remote sensing of aerosol water uptake, *Geophys. Res. Lett.*, 36, L03814, doi:10.1029/2008gl036576, 2009.
- Sheridan, P. J., Jefferson, A., and Ogren, J. A.: Spatial variability of submicrometer aerosol radiative properties over the Indian Ocean during INDOEX, *J. Geophys. Res.*, 107, 8011, doi:10.1029/2000JD000166, 2002.
- Shinozuka, Y., Clarke, A. D., Howell, S. G., Kapustin, V. N., McNaughton, C. S., Zhou, J., and Anderson, B. E.: Aircraft profiles of aerosol microphysics and optical properties over North America: Aerosol optical depth and its association with PM_{2.5} and water uptake, *J. Geophys. Res.*, 112, D12S20, doi:10.1029/2006JD007918, 2007.
- Sorek-Hamer M., Strawa, A. W., Chatfield, R. B., Esswein, R., Cohen, A., and Broday, D. M.: Improved retrieval of PM_{2.5} from satellite data products using non-linear methods, *Environ. Pollut.*, 182, 417–423, 2013.
- Tang, I. N.: Chemical and size effects of hygroscopic aerosols on light scattering coefficients, *J. Geophys. Res.*, 101, 19245–19250, doi:10.1029/96JD03003, 1996.
- Tian, J. and Chen, D. M.: Spectral, spatial, and temporal sensitivity of correlating MODIS aerosol optical depth with ground-based fine particulate matter (PM_{2.5}) across southern Ontario, *Canad. J. Remote Sens.*, 36, 119–128, 2010.
- Tsai, T.-C., Jeng, Y.-J., Chu, D. A., Chen, J.-P., and Chang, S.-C.: Analysis of the relationship between MODIS aerosol optical depth and particulate matter from 2006 to 2008 in Taiwan, *Atmos. Environ.*, doi:10.1016/j.atmosenv.2009.10.006, 2011.
- Twohy, C. H., Coakley, J. A., and Tahnk, W. R.: Effect of changes in relative humidity on aerosol scattering near clouds, *J. Geophys. Res.*, 114, D05205, doi:10.1029/2008JD010991, 2009.
- Van Donkelaar, A., Martin, R. V., and Park, R. J.: Estimating groundlevel PM_{2.5} using aerosol optical depth determined from satellite remote sensing, *J. Geophys. Res.*, 111, D21201, doi:10.1029/2005JD006996, 2006.
- Vidot, J., Santer, R., and Ramon, D.: Atmospheric particulate matter (PM) estimation from SeaWIFS imagery, *Remote Sens. Environ.*, 111, 1–10, 2007.
- Virkkula, A.: Correction of the Calibration of the 3-wavelength Particle Soot Absorption Photometer (3 PSAP), *Aerosol Sci. Technol.*, 44, 706–712, doi:10.1080/02786826.2010.482110, 2010.
- Volkamer, R., Jimenez, J. L., San Martini, F., Dzepina, K., Zhang, Q., Salcedo, D., Molina, L. T., Worsnop, D. R., and Molina, M. J.: Secondary organic aerosol formation from anthropogenic air pollution: Rapid and higher than expected, *Geophys. Res. Lett.*, 33, L17811, doi:10.1029/2006GL026899, 2006.
- Wang, J. and Christopher, S. A.: Intercomparison between satellite derived aerosol optical thickness and PM_{2.5} mass: Implications for air quality studies, *Geophys. Res. Lett.*, 30, 2095, doi:10.1029/2003GL018174, 2003.
- Zhang, Q., Worsnop, D. R., Canagaratna, M. R., and Jimenez, J. L.: Hydrocarbon-like and oxygenated organic aerosols in Pittsburgh: insights into sources and processes of organic aerosols, *Atmos. Chem. Phys.*, 5, 3289–3311, doi:10.5194/acp-5-3289-2005, 2005.
- Ziamba, L., Thornhill, K., Ferrare, R., Barrick, J., Beyersdorf, A., Chen, G., Crumeyrolle, S., Hair, J., Hostetler, C., Hudgins, C., Obland, M., Rogers, R., Scarino, A., Winstead, E., and Anderson, B. E.: Airborne observations of aerosol extinction by in-situ and remote-sensing techniques: Evaluation of particle hygroscopicity, *Geophys. Res. Lett.*, 40, 417–422, 2013.
- Ziamba, L. D., Fischer, E., Griffin, R. J. and Talbot, R. W.: Aerosol acidity in rural New England: Temporal trends and source region analysis, *J. Geophys. Res. Atmos.*, 112, D12S20, doi:10.1029/2006JD007605, 2007.